

# Close-proximity, conservative extrapolation of load spectra

Mirosław Rodzewicz

Faculty of Power and Aeronautical Engineering, Politechnika Warszawska, Warszawa, Poland

## Abstract

**Purpose** – The purpose of this paper is to present the author’s method of conservative load spectrum (LS) derivation and close-proximity LS extrapolation applying a correction for measurement uncertainty caused by too low sampling frequency or signal noise, which may affect the load histories collected during the flying session and cause some recorded load increments to be lower than the actual values.

**Design/methodology/approach** – Having in mind that the recorded load signal is burdened with some measurement error, a conservative approach was applied during qualification of the recorded values into 32 discrete load-level intervals and derivation of  $32 \times 32$  half-cycle arrays. A part of each cell value of the half-cycle array was dispersed into the neighboring cells placed above by using a random number generator. It resulted in an increase in the number of load increments, which were one or two intervals higher than those resulting from direct data processing. Such an array was termed a conservative clone of the actual LS. The close-proximity approximation consisted of multiplication of the LSs clones and their aggregation. This way, the LS for extended time of operation was obtained. The whole process was conducted in the MS Excel environment.

**Findings** – Fatigue life calculated for a chosen element of aircraft structure using conservative LS is about 20%–60% lower than for the actual LS (depending on the applied value of dispersion coefficients used in the procedure of LSs clones generation). It means that such a result gives a bigger safety margin when operational life of the aircraft is estimated or when the fatigue test for an extended operational period is programed based on a limited quantity of data from a flying session.

**Originality/value** – This paper presents a proposal for a novel, conservative approach to fatigue life estimation based on the short-term LS derived from the load signal recorded during the flying session.

**Keywords** Load-spectra, Extrapolation, Unmanned vehicle, Fatigue life

**Paper type** Research paper

## Nomenclature

### Symbols and abbreviations

$AR1, AR2$	= occurrence ratios;
$B$	= dispersion coefficient;
$D$	= fatigue damage (a fraction of life consumed by exposure to series of loads with variable increments);
$FCA$	= symbol of full cycle array (FC-array);
$HCA$	= symbol of half cycle array (HC-array);
$HCA_{add\_st1}$	= a symbol of array to be dispersed and summed with HC-array from flying session;
$HCA_{agg}$ ; $HCA_{agg\_29h}$ array	= symbol of aggregated HCAs from a number of flights (general and supplemented by the information regarding total time of considered set of flights);

$HCA_{env}$	= symbol of envelope of all HC-arrays from all flights;
$HCA_{m+1S}$ ; $HCA_{m+2S}$ ; $HCA_{m+3S}$	= symbol of arrays containing mean values plus 1 or 2 or 3 standard deviations of cells having the same indexes in the set of HCA-arrays derived for each flight;
$HCA_{cCl\_29h}$	= conservative clone of $HCA_{agg\_29h}$ array;
$HCA_{agg\_cCls\_203h}$	= aggregated clones (seven $HCA_{cCl\_29h}$ arrays);
$HCA_{extr\_203h}$	= extrapolated LS for 203h-operational period (rounded number of occurrences);
$HCA_{RFC\_29h}$	= HC-array obtained by application of RFC algorithm to linked load-histories of all flights performed during 29h-flying session;

The current issue and full text archive of this journal is available on Emerald Insight at: <https://www.emerald.com/insight/1748-8842.htm>



Aircraft Engineering and Aerospace Technology  
95/11 (2023) 1–13  
Emerald Publishing Limited [ISSN 1748-8842]  
[DOI 10.1108/AEAT-12-2021-0374]

© Mirosław Rodzewicz. Published by Emerald Publishing Limited. This article is published under the Creative Commons Attribution (CC BY 4.0) licence. Anyone may reproduce, distribute, translate and create derivative works of this article (for both commercial and non-commercial purposes), subject to full attribution to the original publication and authors. The full terms of this licence may be seen at <http://creativecommons.org/licenses/by/4.0/legalcode>

Received 16 December 2021

Revised 21 June 2022

Accepted 4 July 2022

ILS	= incremental load spectrum;
LL	= load level;
LS	= load spectrum;
$\Delta LL$	= load level increment;
$\Delta LL$ -isoline	= a line through HC-array cells of equal LL value;
$n_z$	= load factor;
$\Delta n_z$	= load factor increment;
$N_f$	= number of flights;
P-M	= abbreviation of Palmgren-Miner;
RFC	= Rainflow Counting algorithm;
$\lambda$	= index of load increment; and
$\chi$	= coefficient depending on the type of array used in the modified P-M formula.

**Introduction**

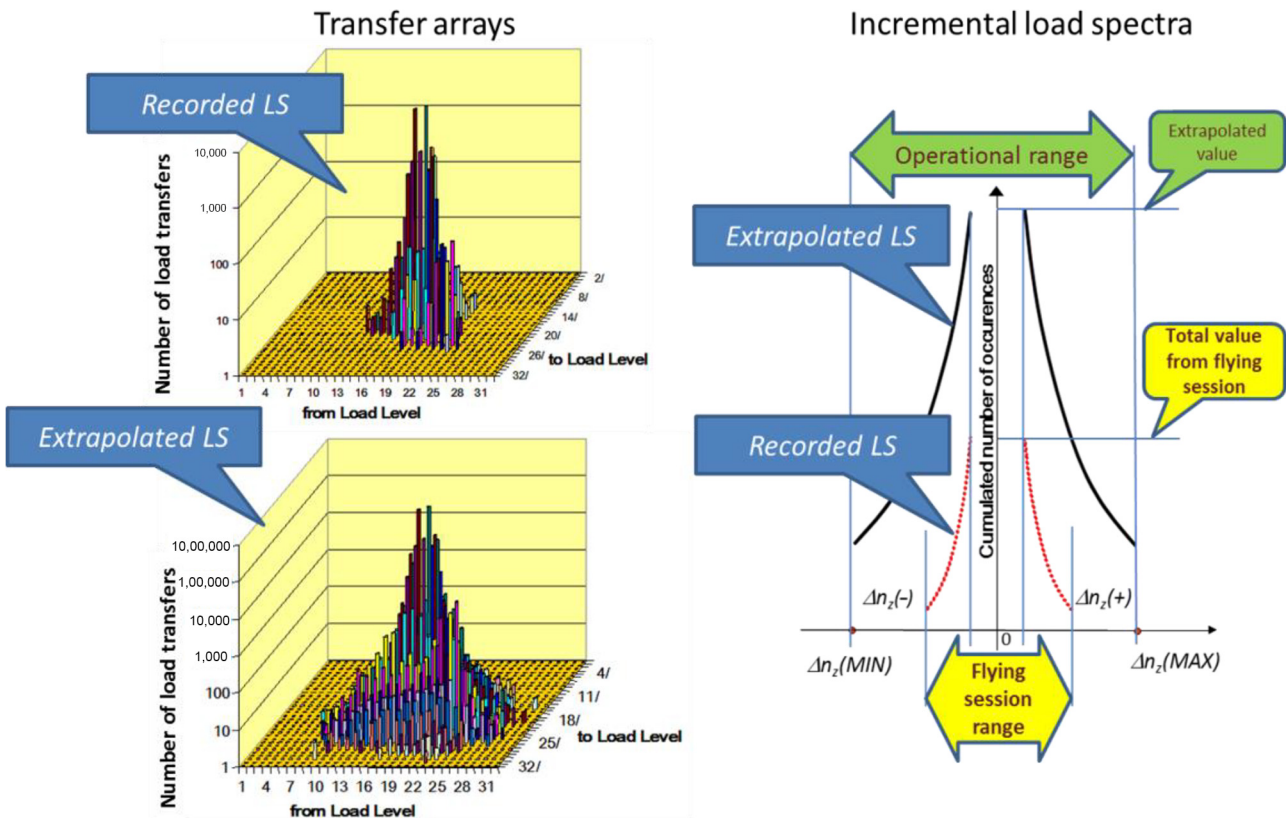
The wide use of unmanned vehicles (Everaerts, 2008; Norasma et al., 2019; Giordan et al., 2020; Goetzendorf-Grabowski et al., 2021) makes the problem of possible safety infringement caused by failures of the unmanned aerial vehicle (UAV) systems increasingly important. As always in aviation, one of the most important problems is strength and fatigue safety of the aircraft structure. Therefore, structure of heavier UAV classes should be investigated for proving their resistance to operational loads (Jin et al., 2013; Rodzewicz,

2012). The aim of this paper is to introduce the author’s method of developing the load spectrum (LS), which can be used in fatigue proof tests. Such a LS should be more conservative than the LS observed during a flying session (i.e. has to produce higher fatigue effect) and should be extended over a longer operational period. The problem of extrapolation of the LS from the short-term version (the LS collected during the flying sessions) to the long-term version (which is necessary to prove the operational life of the device) concerns many fields, such as wind power (Moriarty et al., 2002; Veers and Winterstein, 1998), vehicle (Rui and Wang, 2011) and machinery design (Wang et al., 2011; O’Connor et al., 2002; Yamada et al., 2000) and, particularly, the aerospace (Rodzewicz, 2008; Katcher, 1973).

The problem of extrapolation can be illustrated by Figure 1, which presents both the transformation of a transfer array containing the LS from the flying session and the resulting changes of incremental load spectrum (ILS) (i.e. the multiplied frequencies and extended range of loads in the extrapolated LS).

So far several advanced methods of LS extrapolation have been elaborated (Wang, 2016), including parametric extrapolation methods and, in particular, the Extreme-Value Extrapolation Method (Johannesson, 2006), nonparametric extrapolation methods (Wang et al., 2017; Dressler et al., 1996) and quantile extrapolation methods (Socie and Pompetzki, 2004). Using those methods and based on the results of operational load measurements, various standard LSs (i.e. standardized load sequences) were developed for fatigue proof testing of specific technical devices, like aircrafts, cars, wind-

**Figure 1** Illustration of load spectra extrapolation idea



turbines, etc. (Heuler and Klatschke, 2005). A good example of such a standard LS is KoSMOS (Kollektiv für Segelflugzeuge, Motorflugzeuge bis ca. 2 Abfulgmasse und Motor-Segler), which has been used in Germany for proving fatigue life of composite gliders and light composite aircrafts for about three decades (Kossira and Reinke, 1986).

The method presented in this paper concerns a specific case when loads recorded during a flying session are far from the operational load limits for the aircraft and when collected database is relatively small. Therefore, a hypothetical postulate to extend the LS obtained in such circumstances up to an operational load limit would not be sensible. A much more reasonable postulate is to derive the LS which would be sufficiently conservative to be recognized as a representative LS for the considered case of flying mission (i.e. the LS which provides an extended safety margin in fatigue evaluations). The consideration is focused on photogrammetry mission of PW-ZOOM (Figure 2). It is the UAV constructed at Warsaw University of Technology for the needs of a Polish–Norwegian grant (acronym MONICA). The PW-ZOOM was used in three Antarctic expeditions (2014, 2015 and 2016) flying the total distance of 3.641 km over King George Island. In addition to several thousands of aerial photos, which were used for orthophotomaps creation, also a collection of autopilot logs has been accumulated (Zmarz et al., 2018).

For the analysis presented here, 23 autopilot logs from photogrammetry flights were chosen. Selected statistical data on those flights are shown in Figure 3 together with the GPS traces of all the analyzed flights.

**Analysis of the load spectra gathered during photogrammetry flights of PW-ZOOM over king george island**

Based on acceleration signal written in autopilot logs, the LS was derived for each flight and was written in the form of a  $32 \times 32$  half-cycle array (HC-array), containing in the cell indexed as  $i,j$  the number of load transfers between  $i$  and  $j$  load levels (LL). To obtain such an array, the Rainflow Counting algorithm (RFC) was implemented. The HC-arrays were derived based on the assumed standard relation between LL and load factor  $n_z$ :  $LL = 3$  for  $n_z = 6$  and  $LL = 31$  for  $n_z = -3$  (Głowacki and Rodzewicz, 2014).

The example of such an array is shown in Figure 4, where also a magnified active zone of this array is displayed (i.e. the envelope of all rows and columns having non-zero values). The size of the active zone is the measure of the range of load variation acting during the flight. In the case of this particular flight, the load variation was from  $n_z = -0.11$  up to  $n_z = 4.07$ .

Figure 2 Technical description of the PW-ZOOM – the UAV design for aerial photogrammetry

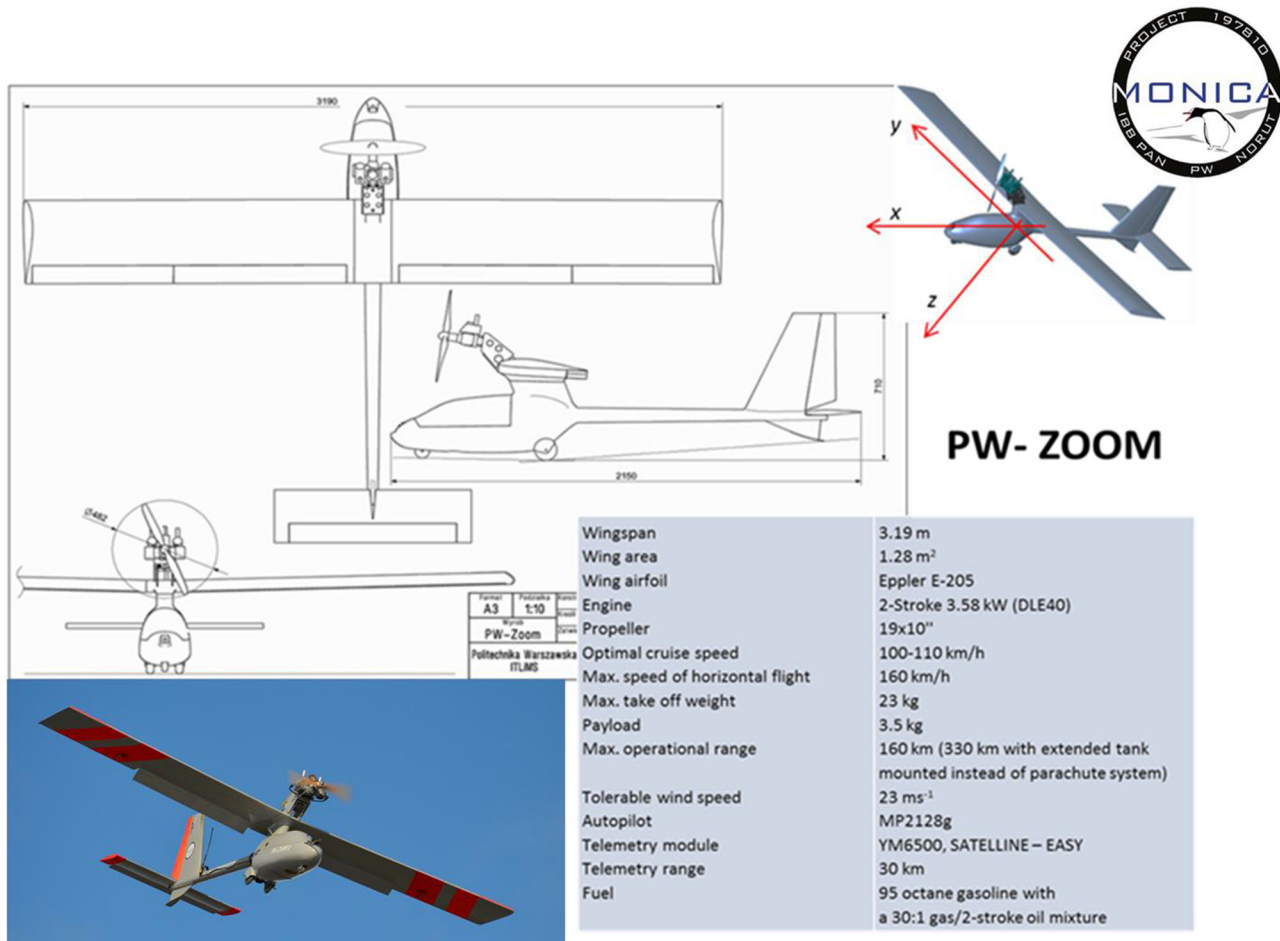
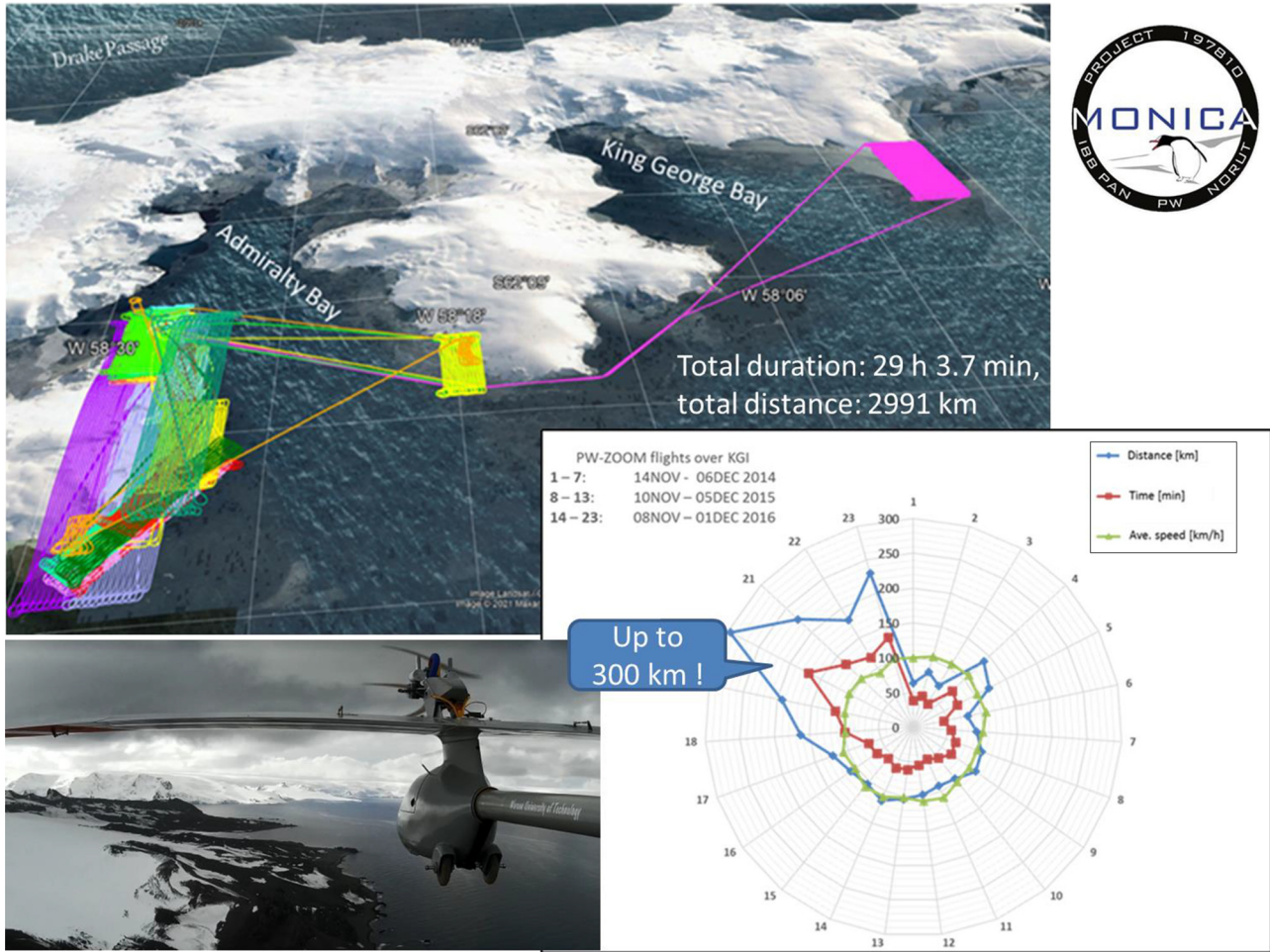


**Figure 3** The set of 23 flight paths of the PW-ZOOM recorded in autopilot logs and the chronological assembly of the PW-ZOOM photogrammetry flights over King George Island



All the HC-arrays presented here concern absolute values of the load increments and contain the summed numbers of half-cycles for positive and for negative load increments. As one can see, they are integers, and their meaning is “number of half-cycles that occurred during the flight.”

Having HC-arrays for all the 23 flights, it was possible to develop an aggregated HC-array labeled as  $HCA_{agg}$ . To do so, it is necessary to sum all arrays. The cell value of the aggregated HC-array can be expressed by an equation (1):

$$hca_{agg,i,j} = SUM(hca(1)_{i,j}; hca(2)_{i,j}; \dots; hca(N_f)_{i,j});$$

where  $N_f = 23$  is the number of flights (1)

As Microsoft Excel was used for calculations, equation (1) contains the symbol of an Excel function. Term SUM means here the summation operation concerning cell values having the same indexes. The same manner is also applied to other formulas. The meaning of the numbers presented in the array is the number of half-cycles that occurred during the 29th flying session; therefore, the symbol of HC-array has been supplemented with this information. It is possible to use the aggregated HC-array for fatigue evaluations, but the result would be not fully trustworthy, because of the load signal

measurement uncertainty. It may cause the load increment written in the HC-array to be lower than the actual value. Looking for a conservative LS, we have to consider a “worse” case (i.e. the LS which may generate higher fatigue damage). Therefore, the series of values of the HC-array cells having the same indexes was subjected to analysis of their variability. The following factors were calculated: the max value, the mean value and the standard deviation. On this basis, the HC-arrays envelope was created. It is an array containing the maxima of values occurring in the set of 23 HC-arrays. Such an envelope is called here  $HCA_{agg\_29h}$  (Figure 5). The cell value of this array can be expressed as: equation (2). In a similar manner, the arrays containing the mean values and standard deviations were also derived [equations (3) and (4)].

$$hca_{env,i,j} = MAX(hca(1)_{i,j}; hca(2)_{i,j}; \dots; hca(N_f)_{i,j}); \quad (2)$$

$$hca_{m,i,j} = AVERAGE(hca(1)_{i,j}; hca(2)_{i,j}; \dots; hca(N_f)_{i,j}); \quad (3)$$

$$hca_{S,i,j} = STDEV.S(hca(1)_{i,j}; hca(2)_{i,j}; \dots; hca(N_f)_{i,j}); \quad (4)$$





defined sampling frequency, so it is possible to miss some peaks of load. Even in completely static conditions, the signal can vary because of the noise. Furthermore, because of the transformation of the measured load signal to discrete LL intervals, the real load signal values which are very near to the next LL interval because of the noise are in fact randomly qualified to one of the neighboring intervals (Figure 7). For these reasons, the results of fatigue calculations may be underestimated. Therefore, based on the observation that the noise is smaller than a single LL interval and applying the conservative approach, it was assumed here that in the case of the HC-arrays obtained from the experiment, the

actual value of any selected cell should be a little bigger, and also, some part of this cell should be moved to the adjoining cells placed 1 or 2 LL intervals higher.

The concept of the conservative LS creation consists of increasing the values of the aggregated HC-array by adding to them a special array obtained as an effect of the dispersion procedure applied to the array being the result of such subtraction: the envelope of HC-arrays minus HC-array for the mean value plus 1 standard deviation. This array is named briefly as the “add-on” array (Figure 8). If one simply adds the “add-on” array to the aggregated HC-array, then he obtains an effect which is shown in Figure 9 regarding the ILS. It is apparent that the LS obtained in this manner is more conservative, but the topology of the resulting array is still the same as in the aggregated HC-array. It means that by adding the “add-on” array, only non-zero values will be increased, but the cells which were empty will also remain empty after this operation.

For that reason, the idea of developing the conservative LS consists in adding to the aggregated HC-array the array obtained by dispersion of the content of the “add-on” array presented in Figure 7. The dispersion schema and the formulas are shown in Figure 10 and equations (5a) and (5b):

$$a_{i-1,j} = a_{i,j} \cdot AR_1 \cdot B \quad (5a)$$

$$a_{i-1,j+1} = a_{i,j} \cdot AR_2 \cdot B \quad (5b)$$

Symbol  $B$  denotes the dispersion factor.  $AR_1$  and  $AR_2$  are the occurrence ratios:

Figure 9 Comparison of incremental load spectra for the HCA\_agg\_29h and the HCA\_agg\_29h integrated with the HCA\_add\_st1

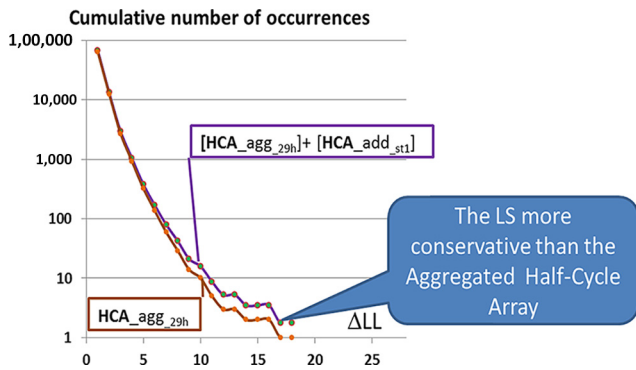
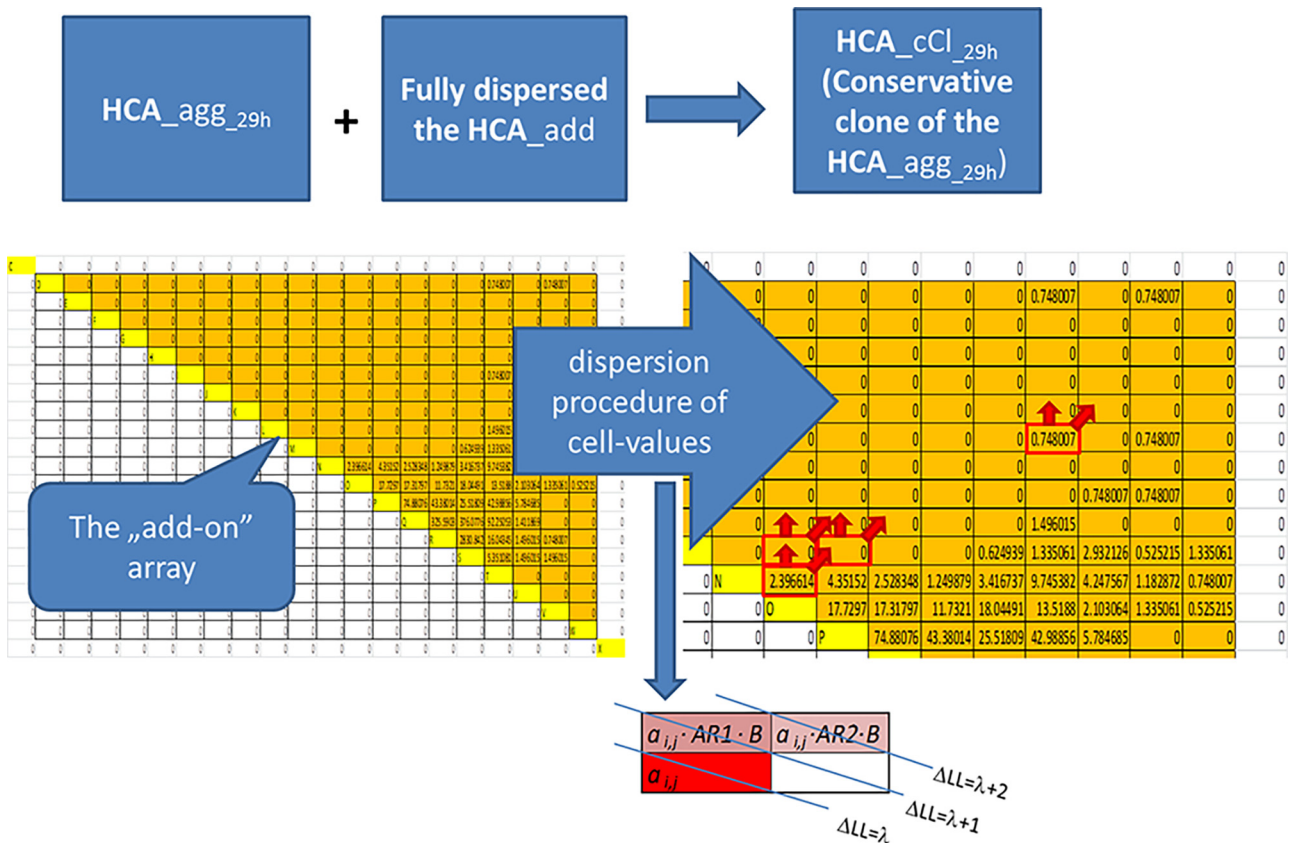


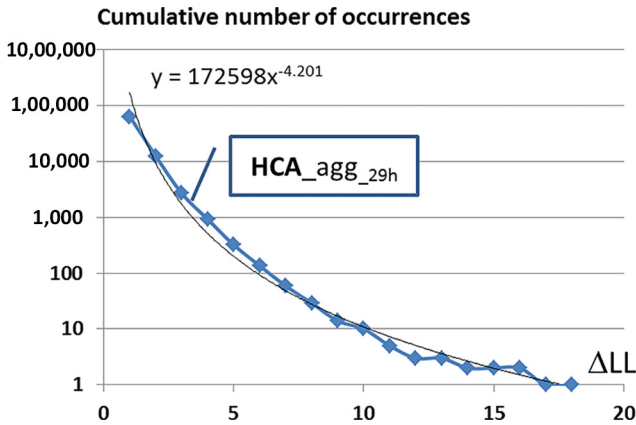
Figure 10 The idea of the conservative clone of the HCA\_agg generation



$$AR_1 = \frac{(\text{the number of half - cycles for } \Delta LL = \lambda + 1)}{(\text{the number of half - cycles for } \Delta LL = \lambda)}; \quad (6a)$$

$$AR_2 = \frac{(\text{the number of half - cycles for } \Delta LL = \lambda + 2)}{(\text{the number of half - cycles for } \Delta LL = \lambda)}; \quad (6b)$$

**Figure 11** Approximation function of the accumulated load spectrum HCA\_agg\_29h



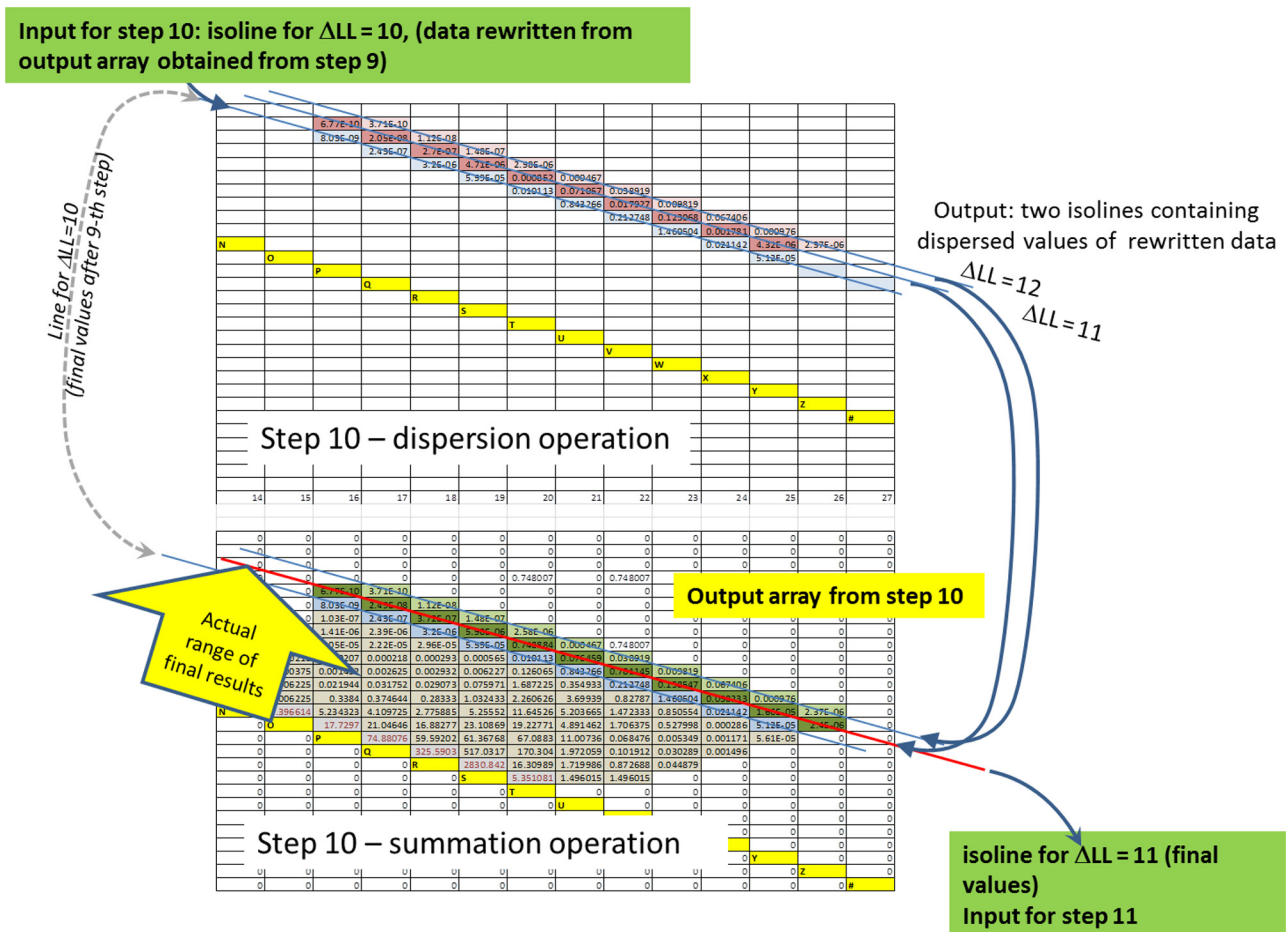
To determine those ratios, the approximation function for incremental LS obtained from the aggregated HC-array was used (Figure 11).

The dispersion procedure of the “add-on” array began from the isoline representing  $\Delta LL = 1$ . The values dispersed on the subsequent isolines representing  $\Delta LL = 2$  and  $\Delta LL = 3$  were then summed with the existing values of the “add-on” array, thus obtaining the input array for the second step of the dispersion procedure, which starts from the next isoline representing  $\Delta LL = 2$ . Such an operation was repeated up to the 22nd step and was stopped when the values dispersed to higher  $\Delta LL$  isolines became very small (lower than  $10^{-4}$ ). Figure 12 illustrates the 10th step of the dispersion procedure.

The process of dispersion was controlled by the factor  $B$ , which determines how much of the cell value is to be dispersed to the higher  $\Delta LL$  isolines. As the signal noise influences mainly the load records, which are located very close to LL intervals borders, it was assumed that this situation may concern 20%–50% of the load signal records. Therefore, the  $B$  variability range was set as  $0.2 \leq B \leq 0.5$ .

Afterwards, two trials were performed for  $B = 0.2$  and  $B = 0.5$ . Each time having fully dispersed the “add-on” array, it was summed with the aggregated HC-array, obtaining in such

**Figure 12** An example of the dispersion process (Step 10 of the procedure)



manner a conservative clone of the LS (labeled as *HCA\_cCl*). As one can see, the conservative clone of the aggregated LS contains values which are slightly magnified and more evenly distributed within the HC-array (Figure 13).

Based on the results of both trials and having in view the stochastic nature of the LSs, it was assumed that in the further proceedings, the dispersion coefficient B will be generated randomly within the range 0.2–0.5.

Figure 13 The *HCA\_agg\_29h* vs *HCA\_cCl\_29h* for  $B = 0.2$

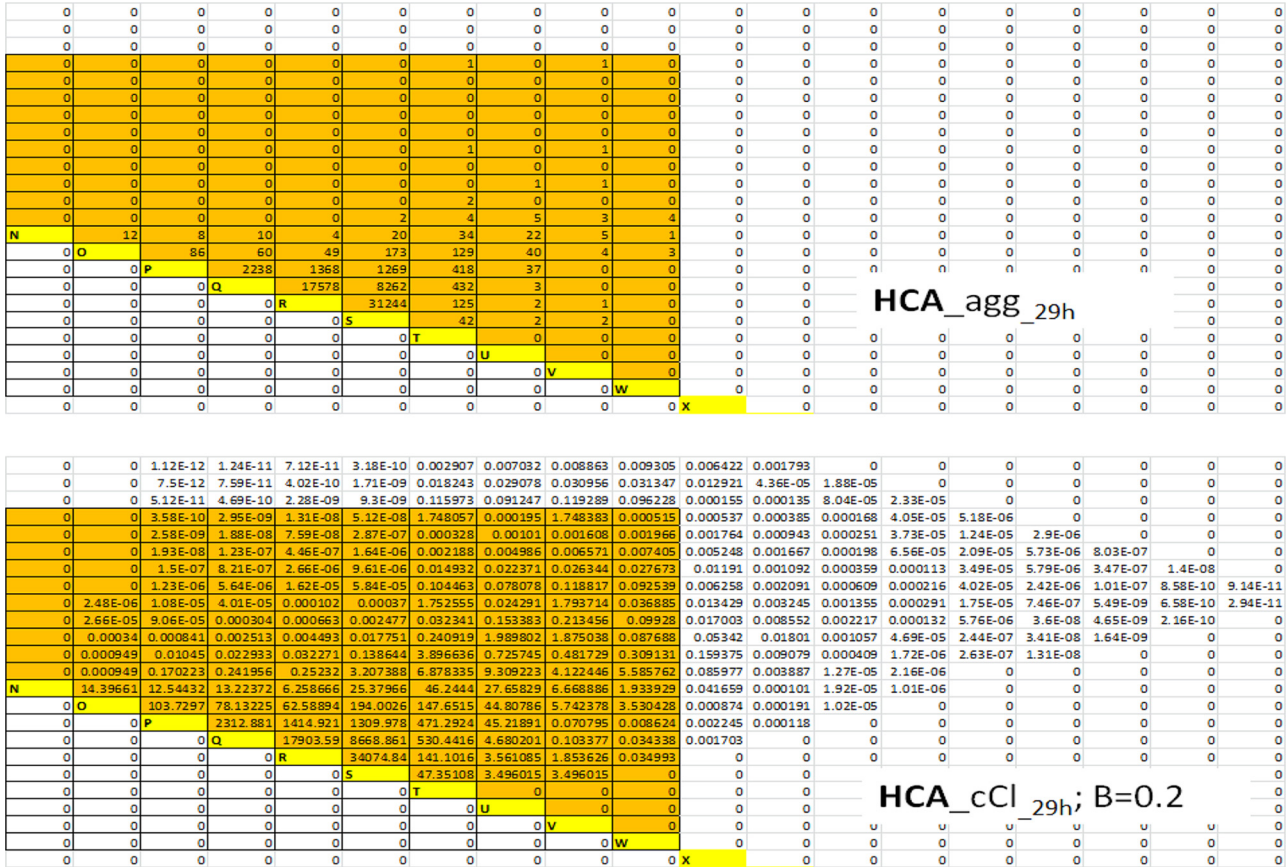
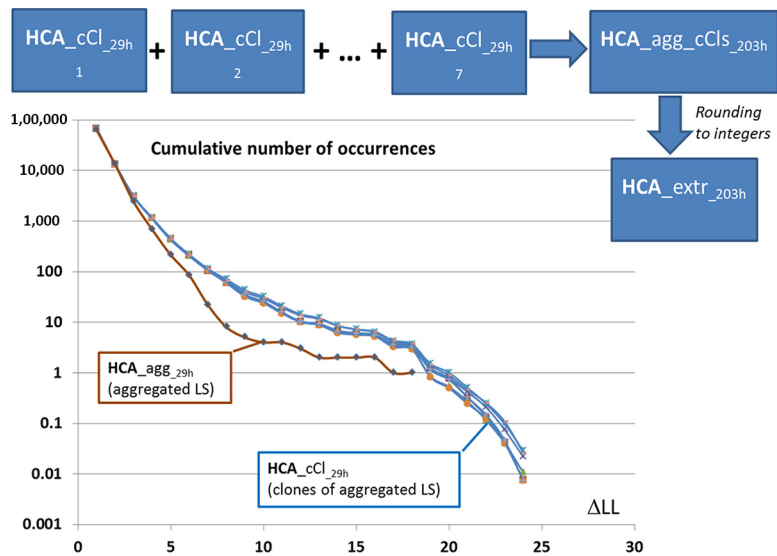


Figure 14 The incremental load spectra derived from the seven clones of the aggregated half cycle array (*HCA\_cCl\_29h*) vs incremental load spectrum for *HCA\_agg\_29h* array



**Close-proximity extrapolation of the load spectrum array**

The dispersion procedure using a randomly generated B factor opens the way to solving also the problem of LS extrapolation. As the database consisting of 23 autopilot logs is rather modest, only a short-range extrapolation can be attempted (named here as “close proximity extrapolation”). To conduct such an operation, it was assumed that up to seven clones will be generated and integrated, giving an operational period extended up to 203 h.

Figure 14 presents the results of the first phase of extrapolation procedure, that is: the ILS derived from seven clones of the aggregated HC-array and the ILS derived solely for the aggregated HC-array (which is added for comparison).

The second phase of extrapolation procedure consists of integration of the aggregated HC-array clones, while the third phase is filtering the cell values by using *ROUND()* function and setting 0 decimal places. The effect of extrapolation described above is apparent on the chart presented in Figure 15. Three-dimensional visualizations of *HCA\_agg\_29h* and *HCA\_agg\_CLS\_203h* are also placed in this Figure, but to show better the extrapolation effect, the number of occurrences was increased ten times.

**Fatigue effect of the conservative load spectrum**

This chapter contains the results of fatigue life calculations for the different LSs described earlier. The calculations were performed for Al-alloy tube used as a wings-fuselage joiner, which was recognized as the element limiting the fatigue life of

the PW-ZOOM primary structure. Fatigue calculations were based on the P-M formula. As the calculations were performed in a domain of transfer arrays, the original P-M formula was modified to the form presented in equation (7).

$$D = \chi \cdot \sum_{i=1}^{32} \sum_{j=1}^{32} D_{ij} = \chi \cdot \sum_{i=1}^{32} \sum_{j=1}^{32} \frac{n_{ij}}{N_{ij}} \quad (7)$$

Symbol  $\chi$  is the coefficient equal to 1 or 0.5 depending on the kind of transfer arrays used for calculations (i.e. a FC-array or a HC-array).

It was assumed that the fatigue properties of the joiner material are like those figured in the chart published in the AFS-120 report (Engineering and Manufacturing Division, 1973). On this basis as well as on the basis of the results of stress variation analysis, the array of load cycles to failure has been drawn up (Figure 16).

The results of fatigue life calculations are presented in Figure 17. Both the fatigue life and the relative fatigue life ratio are displayed. As the reference, fatigue life calculated for the array named as *HCA\_RFC\_29h* was used. This array was obtained by linking together chronologically all the 23 load histories and then applying the RFC procedure.

The following conclusions arise from the presented chart:

- Treating the calculation results for the reference case of LS as the most plausible, it is apparent that the error generated by the use of the aggregated LS (obtained by simple summation of the HC-arrays from each flight) is not significant (the difference of evaluation results is 6%).

**Figure 15** The comparison of the incremental load spectra derived from the HCA arrays for 29 and for 203 h

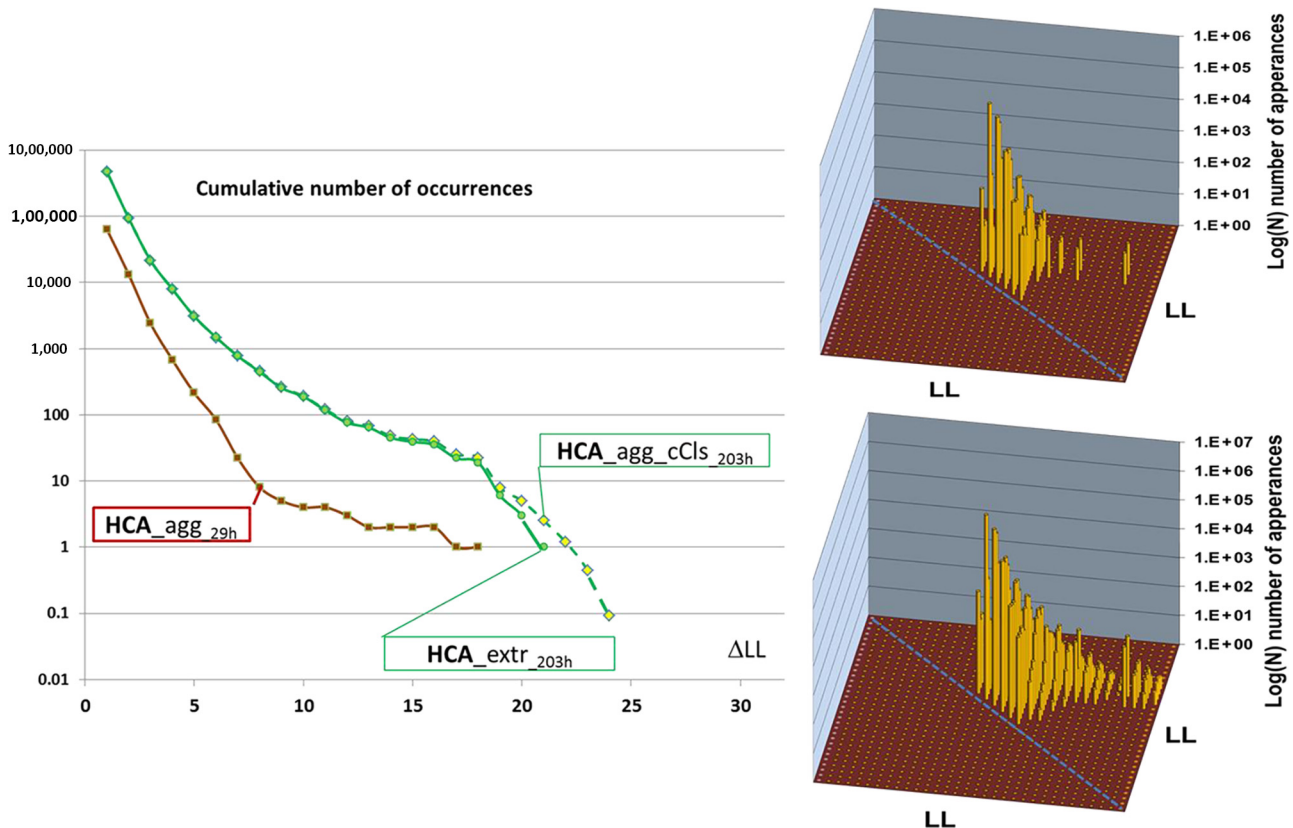
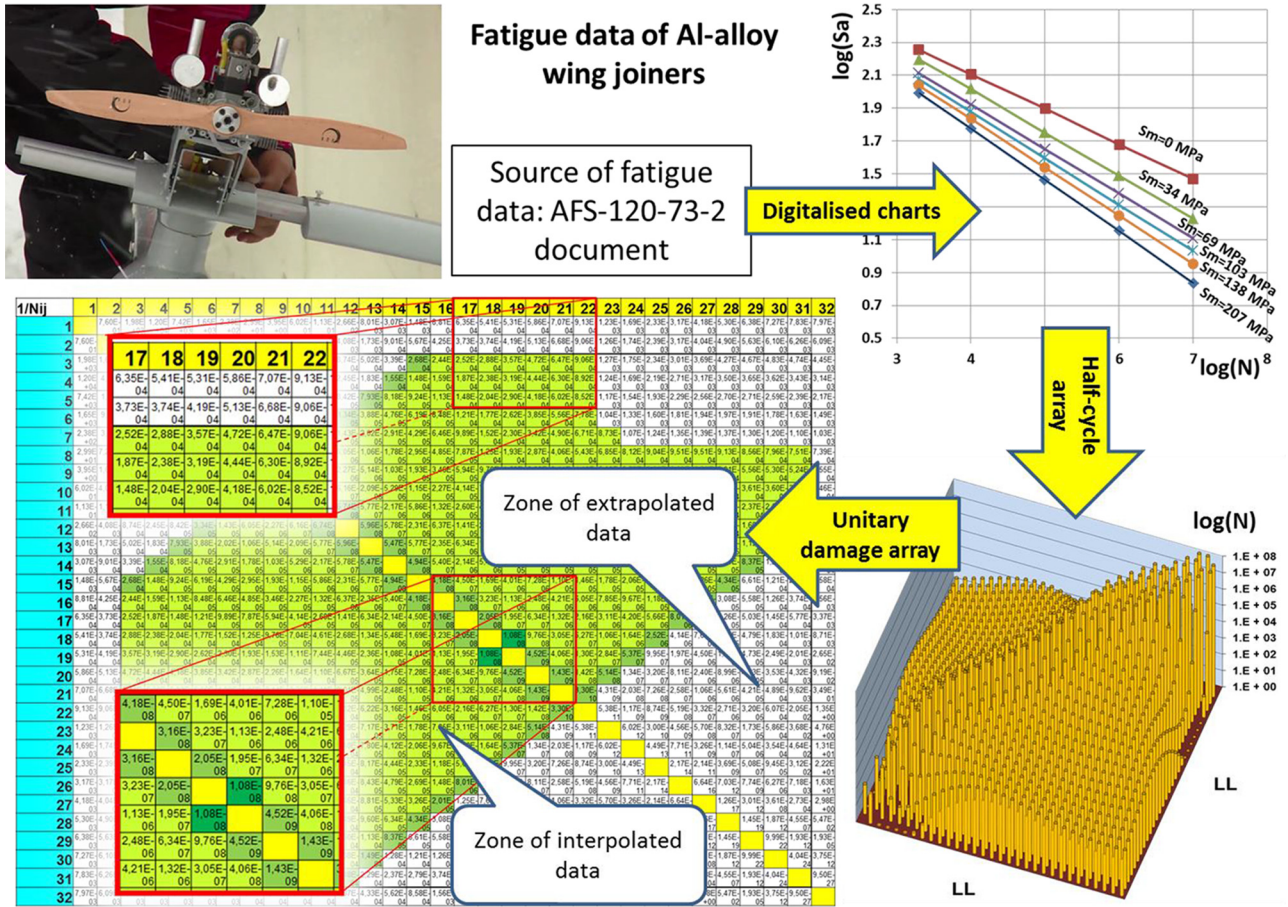


Figure 16 The fatigue properties of the PSE element of the PW-ZOOM's airframe



life (see the bars labeled as v1 and v2); nevertheless, the effect of using a random number generator is visible.

- The use of *ROUND()* function gives a noticeable effect regarding the topology of the extrapolated HC-array, but fortunately, it does not have a large influence on the result of fatigue life calculation (i.e. it gives more optimistic results of about 4% in comparison with the result calculated from the non-filtered HC-array derived for extrapolated LS).

## Conclusions

The obtained results of the calculations based on conservative clones of the LS seem logical.

The conservative LS generates a higher fatigue, as a result giving a reduction of fatigue life of about 24%–62% (depending on the dispersion factor) in comparison with the LS derived directly from the load signal recorded during a flying session. This gives a bigger safety margin when the service life for the UAV structure is evaluated. The research contributes to the increase in the safety of using unmanned aerial vehicles. In the situation of the growing number of applications of unmanned aviation operating in urbanized areas, it is a very important matter.

The method presented here needs further verification work, especially regarding the range of the dispersion factor variability. The range assumed here, namely, 0.2–0.5 (covering the range between the optimistic and the pessimistic assessment), needs verification. For this purpose, it would be necessary to continue with new sessions of photogrammetric flights. Collecting data over the same operational period as the one selected for the extrapolation described in this paper would allow a full verification of both the conservative LS clones generation and the LS close-proximity extrapolation methods.

## References

- Dressler, K., Gründer, B., Hack, M. and Köttgen, V.B. (1996), “Extrapolation of rainflow matrices”, SAE Technical Paper 960569.
- Everaerts, J. (2008), “The use of unmanned aerial vehicles (UAVS) for remote sensing and mapping”, *The International Archives of the Photogrammetry, Remote Sensing and Spatial Information Sciences*, Vol. XXXVII No. Part B1, pp. 1187-1191.
- Giordan, D., Adams, M.S., Aicardi, I., Alicandro, M., Allasia, P., Baldo, M., De Berardinis, P., Dominici, D., Godone, D., Hobbs, P., Lechner, V., Niedzielski, T., Piras, M., Rotilio, M., Salvini, R., Segor, V., Sotier, B. and Troilo, F. (2020), “The use of unmanned aerial vehicles (UAVs) for engineering geology applications”, *Bulletin of Engineering Geology and the Environment*, Vol. 79 No. 7, pp. 3437-3481.
- Głowacki, D. and Rodzewicz, M. (2014), “Investigation into load spectra of UAVS aircraft”, *Fatigue of Aircraft Structures*, Vol. 2013 No. 5, pp. 40-52.
- Goetzendorf-Grabowski, T., Tarnowski, A., Figat, M., Mieloszyk, J. and Hernik, B. (2021), “Lightweight unmanned aerial vehicle for emergency medical service – synthesis of the layout”, *Proceedings of the Institution of Mechanical Engineers, Part G: Journal of Aerospace Engineering*, Vol. 235 No. 1, pp. 5-21.
- Heuler, P. and Klatschke, H. (2005), “Generation and use of standardised load spectra and load–time histories”, *International Journal of Fatigue*, Vol. 27 No. 8, pp. 974-990.
- Jin, G.D., Lu, L.B., Gu, L.X., Liang, J. and Zhu, X.F. (2013), “Fatigue life of UAV airframe based on damage coefficient”, *Advanced Materials Research*, Vol. 709, pp. 358-362.
- Johannesson, P. (2006), “Extrapolation of load histories and spectra”, *Fatigue & Fracture of Engineering Materials and Structures*, Vol. 29 No. 3, pp. 209-217.
- Katcher, M. (1973), “Crack growth retardation under aircraft spectrum loads”, *Engineering Fracture Mechanics*, Vol. 5 No. 4, pp. 793-818.
- Kossira, H. and Reinke, W. (1986), “Entwicklung eines belastungskollektivs für leichte motorflugzeuge aus den beanspruchungsmessungen an einem segelflugzeug”, IFL-IB 86-04, TU Braunschweig.
- Moriarty, P.J., Holley, W.E. and Butterfield, S. (2002), “Effect of turbulence variation on extreme loads prediction for wind turbines”, *Journal of Solar Energy Engineering*, Vol. 124 No. 4, pp. 387-395.
- Norasma, C.Y.N., Fadzilah, M.A., Roslin, N.A., Zanariah, Z. W.N., Tarmidi, Z. and Candra, F.S. (2019), “Unmanned aerial vehicle applications in agriculture”, IOP conf”, *Ser.: Materials Science and Engineering*, Vol. 506, p. 012063.
- O’Connor, A., Caprani, C. and Belay, A. (2002), “Site-specific probabilistic load modeling for bridge reliability analysis”, *Assessment of Bridges and Highway Infrastructure*, pp. 97-104.
- Rodzewicz, M. (2008), “Determination and extrapolation of the glider load spectra”, *Aircraft Engineering and Aerospace Technology*, Vol. 80 No. 5, pp. 487-496.
- Rodzewicz, M. (2012), “Airworthiness tests of the UAV structure – fatigue issues”, *Fatigue of Aircraft Structures*, Vol. 2012 No. 4, pp. 82-93.
- Rui, Q. and Wang, H.Y. (2011), “Frequency domain fatigue assessment of vehicle component under random load spectrum”, *Journal of Physics: Conference Series*, Vol. 305 No. 1, pp. 1-9.
- Socie, D. and Pompetzki, M. (2004), “Modeling variability in service loading spectra”, *Journal of ASTM International*, Vol. 1 No. 2, pp. 46-57.
- Veers, P.S. and Winterstein, S.R. (1998), “Application of measured load to wind turbine fatigue and reliability analysis”, *Journal of Solar Energy Engineering*, Vol. 120 No. 4, pp. 233-239.
- Wang, J., Li, Y. and Jiang, Z. (2017), “Non-parametric load extrapolation based on load extension for semi-axle of wheel loader”, *Advances in Mechanical Engineering*, Vol. 9 No. 3, pp. 1-12.
- Wang, J., Chen, H., Li, Y., Wu, Y. and Zhang, Y. (2016), “A review of the extrapolation method in load spectrum compiling”, *strojniški vestnik*, *Journal of Mechanical Engineering*, Vol. 62 No. 1, pp. 60-75.
- Wang, J.X., Liang, Y.L., Wang, Z.Y., Wang, N.X., Yao, M.Y. and Sun, Y.F. (2011), “Test and compilation of load spectrum of hydraulic cylinder for earth moving machinery”, *Advanced Science Letters*, Vol. 4 No. 6, pp. 2022-2026.
- Yamada, K., Cao, Q. and Okado, N. (2000), “Fatigue crack growth measurements under spectrum loading”, *Engineering Fracture Mechanics*, Vol. 66 No. 5, pp. 483-497.
- Zmarz, A., Rodzewicz, M., Dąbski, M., Karsznia, I., Korczak-Abshire, M. and Chwedorzewska, K.J. (2018), “Application of UAV BVLOS remote sensing data for

multi-faceted analysis of antarctic ecosystem”, *Remote Sensing of Environment*, Vol. 217, pp. 375-388.

### **Further reading**

Engineering and Manufacturing Division, Airframe Branch (1973), “Fatigue evaluation of wing and associated structure

on small airplanes”, Report No. AFS-120-73-2, sponsored by Department of Transportation, Federal Aviation Administration, Washington, DC.

### **Corresponding author**

**Mirosław Rodzewicz** can be contacted at: [miro@meil.pw.edu.pl](mailto:miro@meil.pw.edu.pl)